Integrated evaporator-condenser cascaded adsorption system for low temperature cooling using different working pairs

Dakkama, Hassan; Elsayed Ali Hussin, Ahmed; Al-Dadah, Raya; Mahmoud, Saad; Youssef, Peter

DOI:
10.1016/j.apenergy.2016.01.132

Document Version
Peer reviewed version

Citation for published version (Harvard):
Dakkama, H, Elsayed Ali Hussin, A, Al-Dadah, R, Mahmoud, S & Youssef, P 2016, 'Integrated evaporator-condenser cascaded adsorption system for low temperature cooling using different working pairs', *Applied Energy*. https://doi.org/10.1016/j.apenergy.2016.01.132

Integrated Evaporator-Condenser Cascaded Adsorption System for Low Temperature Cooling Using Different Working Pairs

H.J. Dakkama [a,b,c*], A. Elsayed [a,d], R.K. AL-Dadah [a], S.M. Mahmoud [a], P. Youssef [a]

[a] *School of Mechanical Engineering, University of Birmingham, Birmingham, B15 2TT, United Kingdom.*

[b] *Engineering Technical College-Baghdad, Middle Technical University, Baghdad, Iraq.*

[c] *The Higher Committee for Education Development in Iraq.*

[d] *Mechanical Engineering Department, Alexandria University, Egypt.*

* Corresponding author email: hassan_jfsd@yahoo.com ; tel.: 00447405794147.

Abstract

A cascaded adsorption cooling system with an integrated evaporator/condenser can produce low temperature cooling, using waste heat sources. The choice of the working pair in such a system affects the system's performance when driven by low temperature waste heat sources, which can be as low as 70^{o}C. This paper investigates the performance of various adsorbent/refrigerant working pairs in a cascaded adsorption system with an integrated evaporator/condenser using Simulink/MATLAB software. The cascaded system consists of two pairs of adsorber beds, a condenser, an evaporator and an integrated condenser/evaporator heat exchanger, forming upper and bottoming cycles. Five combinations of working pairs were investigated: ATO/ethanol + Maxsorb/R507A; Maxsorb/R134a + Maxsorb/propane; ATO/Ethanol + Maxsorb/propane; ATO/ethanol +AC-35/methanol; and Maxsorb/R134a + Maxsorb/R507A. The latter combination was used for validation and as a reference combination for assessing the performance of the investigated working pairs in terms of COP and cooling capacity. The results showed that the Maxsorb/R134a + Maxsorb/propane combination gives a higher COP compared to the reference combination, with up to 30.0% and 30.1% for the COP and cooling capacity, respectively; while ATO/ethanol +AC-35/methanol produces a similar performance to the reference case but uses natural refrigerants with low global warming potential and low cost adsorbent materials.

Keywords: Adsorption; Cascading; Working Pairs; Freezing; Simulink.

This paper was presented at the 7th International Conference on Applied Energy (ICAE2015), March 28-31, 2015, Abu Dhabi, UAE (Original paper title: " Investigation of Cascading Adsorption Refrigeration System with Integrated Evaporator-Condenser Heat Exchanger Using Different Working Pairs" and Paper No.: 381).

Nomenclature

A	Area, [m^2]	*U*	Overall heat transfer coefficient, [$W/m^2/K$]
*C*p	Specific heat, [kJ/kg/K]	*x*	Instantaneous uptake, [kg_{ref}/kg_{ads}]
COP	Coefficient of Performance, [-]	x_o	Actual uptake [kg_{ref}/kg_{ads}]
Dso	Pre-exponential constant, [m^2/s]	**Subscript**	
*E*a	Activation energy, [kJ/kg]	AC	Activated carbon (adsorbent)
*F*p	Particle shape factor [-]	ads	Adsorption
h	Enthalpy, [kJ/kg]	Al	Aluminum
ksav	Overall mass transfer coefficient, [1/s]	bed	Adsorber bed
m	Characteristic energy of the system,[kJ/kg]	cond	Condenser
$\dot{m}$	Mass flow rate, [kg/s]	Cu	Copper
n	Heterogeneity parameter, [-]	des	Desorption
Q	Heat power, [kW]	evap	Evaporator
Qst	Isosteric heat of adsorption, [kJ/kg]	g	Gas
P	Pressure [kPas]	heating	Heating at desorption and switching time
R	Universal gas constant=8.314, [J/mol/K]	hot	Hot heat transfer source
*R*p	Adsorbent particle radius, [m]	in	Inlet
SCP	Specific Cooling Power [W/kg]	ref	Refrigerant (adsorbate)
T	Temperature, [K]	S	Saturation
t	Time, [sec]	w	Water

1. Introduction

Globally, there is a significant amount of waste heat emitted from power plants operating at an efficiency ranging from 30-50% [1-3]; a significant amount of this waste heat has a temperature below 100^{o}C [4-5]. Adsorption and absorption refrigeration technologies can be used to exploit this waste heat to produce cooling; thus reducing fossil fuel consumption and CO_2 emissions. Despite the performance of absorption refrigeration systems (0.045 [6] and 0.33 [7]) being higher than that of the adsorption systems, they do

have some drawbacks, such us: contamination, crystallization and corrosion [8-10]. Adsorption cooling technology offers advantages in terms of stability and the use of environmentally friendly working pairs [11], but suffers from lower COP compared to absorption systems. The cascading of adsorption systems is one of the improvement techniques that has been reported to enhance the COP of intermittent and two-bed cycles by 60% and 50% [12-14]. In cascaded adsorption systems, the COP and SCP can be further improved by using an integrated evaporator/condenser integrated into two cycles in which more than one bed is used to generate continuous cooling. Habib [15] presented a performance analysis of a four-bed adsorption refrigeration system, formed from two systems with different working pairs; where the upper system used activated carbon/R134a and the lower system used activated carbon/R507A. The aim of this work was to provide refrigeration load at a low temperature of -10^{o}C using a low desorption temperature of 70^{o}C. The effect of the cycle time, switching time, bed and brine temperatures on the COP, cooling capacity and chiller efficiency were investigated to determine the optimum operating conditions. Meunier [16] theoretically studied the performances of four configurations of cascading adsorption refrigeration systems at different generation and evaporation temperatures. To achieve a low evaporator temperature of -10^{o}C, a system with four adsorbers, two condensers and two evaporators was recommended. Two adsorber beds were packed with zeolite-water and the other two beds were packed with activated carbon-methanol. The two cycles were amalgamated using the double effect technique where their adsorbers were thermally connected for exchanging heat through thermal storage reservoirs. Moreover, the reservoir of the activated carbon-methanol adsorption cycle was connected with the water evaporator for exchanging heat. High and medium desorption temperatures up to 275 and 110^{o}C were required to drive the zeolite-water and activated carbon- methanol cycles, respectively. Dawoud [17] developed a theoretical analysis of a hybrid solar-adsorption refrigeration system where two adsorption cycles were combined to achieve low temperature refrigeration for vaccine storage. Zeolite-13X and SWS-2L were packed in the adsorbers as an adsorbent and water was used as a refrigerant. The operating conditions for the zeolite and SWS-2L cycles were assumed to be desorption and evaporator temperatures of 280 and

122°C and -5 and -5°C, respectively. Solar energy was used to drive the SWS-2L cycle while the gas burner was used to operate the zeolite cycle.

Oliveira [18] carried out an experimental study of an adsorption icemaking system consisting of four beds, a condenser and an evaporator arranged in a two-stage cycle using an activated carbon/ammonia working pair. Tests were carried out at a desorption temperature ranging from 85 to 115°C and evaporation temperature down to -27°C. Wang [19] experimentally built a double stage adsorption freezing unit using three levels of heat source temperatures of 75, 80 and 85°C; each level was tested at three average values of the evaporator's outlet temperature of -5, -10 and -15°C. The chemical adsorbents ($CaCl_2$ and $BaCl_2$) and ammonia were used as the working pair. The condenser temperature was up to 25°C. The system developed by Wang was amalgamated by Jiang [20] with Organic Rankin Cycle to utilize the waste heat to drive the two cycles using a cascading technique. The same chemical salt was used as an adsorbent but with ethanol as a refrigerant. The double stage adsorption freezing cycle was driven at a generation and condensing temperature up to 90 and 30°C, respectively.

The previously described literature on adsorption refrigeration systems for producing cooling below 0°C have indicated that these systems utilised either chemical adsorbents (not stable with time), toxic refrigerant (ammonia) high desorption temperature, toxic refrigerant, chemical solid sorbents (not stable with time) or the kinetic equation for dry sample (not cyclic). Also when utilising low temperature waste heat sources, global warming refrigerants were used. However, there is no clear comparison available in the literature regarding the selection of working pairs suitable for a low evaporating temperature, a high condensing temperature and a low desorption temperature, where low temperature heat sources can be used. Therefore, this work investigates five combinations of adsorbent/refrigerant pairs, namely; ATO/ethanol + Maxsorb/R507A; Maxsorb/R134a + Maxsorb-propane; ATO/ethanol + Maxsorb/propane, Maxsorb/R134a + Maxsorb/R507A; and ATO/ethanol + AC-35/methanol, for low temperature cooling using low temperature heat sources. Such pairs have been reported to have good adsorption characteristics

and be suitable for low temperature cooling; thus they can produce an energy efficient adsorption system for ice making [15, 21-23]. Simulink software was used to solve the differential equations representing the cascaded adsorption system linked with the Refprop package, to utilise the thermo-physical properties of different fluids.

2. Materials and Methods

2.1 Working Pair Selection

The selection of the working pair is critical to achieve an efficient adsorption ice-making system. Ammonia is the most commonly used refrigerants for low temperature adsorption systems due to its high adsorption capabilities and being a natural refrigerant, with no ozone depleation and a low global warming potential and good thermal properties [5]. However it is a toxic refrigerant and extra health and safety measures are required. Ethanol is a non-toxic refrigerant, ozone-friendly with a freezing point up to -114^0C; it has a good affinity with various activated carbons [24]. Propane (R-290) also has zero Ozone Depletion Potential (ODP); it is not toxic and has a low normal boiling point up to -42.114^0C, as well as its remarkable thermal properties which naturally exist with low cost [22]. Regarding the adsorbent, activated carbon is chosen as a physical adsorbent due to its stability and reliability, compared to the chemical adorbents. Maxsorb, ATO and AC-35 are used in this work, where Maxsorb is an advanced activated carbon with high ethanol adsorption capabilities (1.18 kg/kg) compared to ATO (0.4 kg/kg) [21] while ATO and AC-35 have a considerably lower cost than Maxsorb. The ATO and AC-35 are 62.5 and 7.2 times cheaper than the Maxsorb [25].

2.2 Working Principle

Fig. 1 shows the main and secondary components of the adsorption refrigeration system consisting of four adsorbers (two adsorbers driven by a high temperature heat source (HDT) and two adsorbers driven by a low temperature heat source (LDT)); a condenser, an evaporator and Integrated Evaporator-Condenser Heat Exchanger (IECHE). Two adsorbers are prepared to work as the upper stage (1^{st} stage) using one

type of working pair and the other two adsorbers are charged with a different type of working pair to operate as the bottom stage (2^{nd} stage). The adsorbers of the 1^{st} stage are connected with the condenser and the IECHE; while the adsorbers of the 2^{nd} stage are linked with the IECHE and the evaporator. Therefore the IECHE simultaneously works as an evaporator and condenser for the 1^{st} and 2^{nd} stages, respectively. The use of the ICEHE reduces the complexity of the system and enhances the heat transfer rate by utilising the conduction, convection and phase change processes for both mediums within the IECHE. The cooling capacity is produced only by the evaporator of the 2^{nd} stage. The total cycle time is divided into four modes; in Mode 1, the HDT1 and LDT1 adsorbers are heated up by circulating hot water through them during preheating process, while the HDT2 and LDT2 adsorbers are precooled by circulating cold water. This mode is just applied during the switching time where there is no refrigerant flowing to the condenser, ICEHE and evaporator. In Mode 2, the heating process continues through the HDT1 and LDT1 adsorbers to start the desorption-condensation processes by connecting them with the condenser and ICEHE, respectively. The HDT2 and LDT2 adsorbers continue to be cooled but they will be linked with the ICEHE and the evaporator respectively, to begin the adsorption-evaporation processes. In Mode 3 and 4 the processes of the HDT1 and LDT1 adsorbers in Mode 1 and Mode 2 are swapped those of with HDT2 and LDT2 and vice versa. The ICEHE enables using the latent heat of condensation

of the stage 2 refrigerant to supply the heat of evaporation of the stage 1 refrigerant; thus no secondary fluids are needed.

Fig.1. Description of the main components of an adsorption refrigeration system with ICEHE

3. Simulink Modelling for Cascading Adsorption Refrigeration System

The ordinary differential Equations 1-12, which describe the thermal performance of the adsorber beds, condenser, evaporators and the ICEHE, have been used to simulate the dynamic response using Simulink/ MATLAB to determine condensation, evaporation, desorption, adsorption temperatures and cyclic uptake of refrigerants in upper and bottoming cycles using different working pairs. Detailed information about the various components of the adsorption system including the mass of the adsorbent materials, the mass of metal and overall heat transfer coefficients, are taken from Habib [15] and summarized in Table 1.

Table 1

Initial and standard values, as given in [11,15-17]

Symbols	Value	Units	Symbols	Value	Units
$\dot{m}_{w,ads/des/cond}$	0.3	kg/s	$(Q_{st})_{Maxsorb-Ethanol}$	1050	kJ/kg
$\dot{m}_{Brine}$	0.1	kg/s	m_{AC}	50	kg
$T_{w,in,des}$	70	°C	$m_{ref\ cond}$	25	kg
$T_{w,in,cond}$	30	°C	$m_{ref\ evap}$	13	kg
$T_{w,in,des}$	50	°C	m_{Al}	64	kg
$T_{Brine,in}$	-5	°C	m_{Cu}	20.3	kg
$(UA)_{bed}$	3000	J/K	Cp_{AC}	0.93	kJ/(kg.K)
$(UA)_{evap}$	4770	J/K	Cp_{Al}	0.904	kJ/(kg.K)
$(UA)_{cond}$	15300	J/K	Cp_{Cu}	0.386	kJ/(kg.K)
$(Q_{st})_{Maxsorb-R134a}$	215	kJ/kg	Cp_{Brine}	3.4	kJ/(kg.K)
$(Q_{st})_{Maxsorb-R507A}$	265	kJ/kg	Half cycle time	540	sec

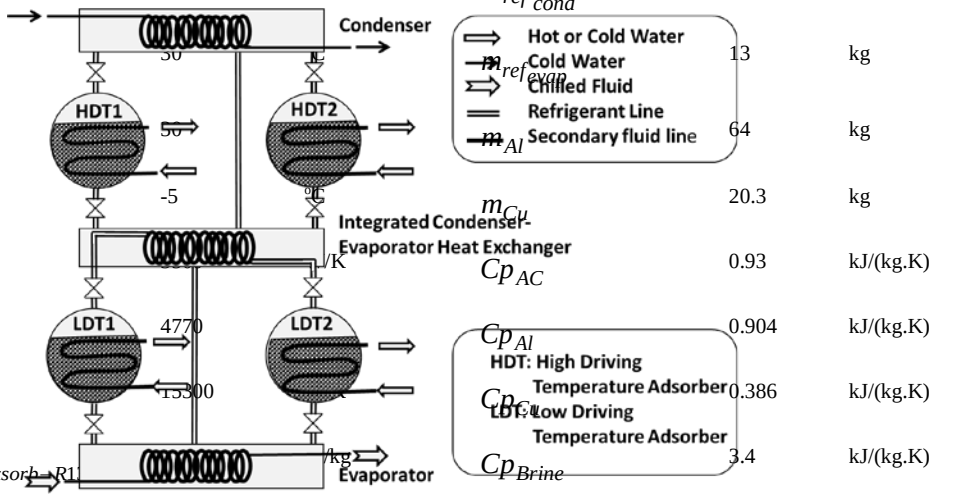

$(Q_{st})_{Maxsorb-propane}$	450	kJ/kg	Switching time	50	sec

The equilibrium uptake of refrigerant on the adsorbent material is estimated using the Dubinin-Astakov (D-A) isotherm model as [26]:

$$x_{eq} = x_o \exp\left(-\left(R.T \ln\left(P_s / P\right)/ m\right)^n\right) \quad (1)$$

R is the universal gas constant (8.314 J/mol/K); T is the local temperature inside the adsorber; P_s is the refrigerant vapour pressure corresponding to the adsorber temperature while P is the vapour pressure at the condenser's or evaporator's condition relating to the desorption or adsorption mode, respectively.

The adsorption/desorption rates for different working pairs are calculated using the linear driving force theory (LDF) [21, 23, 27], as given by:

$$dx / dt = \left(F_p D_{so} / {R_p}^2\right) \times \exp\left(-E_a /(RT)\right) \times \left(x_{eq} - x\right) \quad (2)$$

Table 2 presents the empirical values of different working pairs required for Equations 1 and 2.

Table 2

Empirical parameters of adsorption isotherm [15, 21- 23, 27- 28]

	E_a (J/mol)	R_p (m)	F_p.D_{so}/R_p^2	D_{so} (m^2/s)	x_o (kg/kg)	n	F_p	k_{sav} (1/s)
Maxsorb-Ethanol:	40276.718	95×10^{-6}	7175.344	_	1.12934	2.3169	_	_
ATO-Ethanol:	47830	365.1×10^{-6}	187423.9	_	0.4368	2.3169	_	_
Maxsorb-Propane:	_	_	_	_	0.96	1.220.	_	006395
Maxsorb-R134a:	7332.69	36×10^{-6}	_	1.44×10-1	2.22	1.29	9.8596	_
Maxsorb-R507A:	7547.24	36×10^{-6}	_	3.41×10-11	2.05	1.34	9.8596	_
Ac-35-Methanol	7960	_	$7.35*10^{-3}$	_	0.425	2.15	_	_

For each adsorber bed of the upper and bottom cycles, the energy balance is applied to determine the temperature variations with time as:

$$\left(m_{AC}\left(C_{p_{AC}}+C_{p_{ref}}.x\right)+m_{Al}.C_{p_{Al}}+m_{Cu}.C_{p_{Cu}}\right)\frac{dT_{ads/des}}{dt}=\delta m_{AC}\left[h_g\left(P_{evap/cond},T_{ads/des}\right)-h_g\left(T_{evap/cond}\right)+Q_{st}\right]\frac{dx_{ads/des}}{dt}+\dot{m}_{w,ads/des}C_{p_w}\left(T_{w,in,ads/des}-T_{w,out,ads/des}\right) \quad (3)$$

The log mean temperature difference (LMTD) is used to evaluate the outlet temperature of water as given by:

$$T_{w,out,ads/des}=T_{bed}+\left(T_{w,in,bed}-T_{bed}\right)\exp\left(-(UA)_{bed}/\left(\dot{m}.C_p\right)_w\right) \quad (4)$$

The switching signal (δ) was applied in the mathematical model in order to enable and disable the adsorption or desorption process where δ = 1 during adsorption or desorption time and takes a value of zero during the switching period. The left-hand side of Eqution (3) consists of four terms: the internal energy of the adsorbate, adsorbent, the copper tube metal of heat exchanger bed and the aluminium fins metal. The first term on the right hand side evaluates the heat energy that is added or removed during the desorption or adsorption period, respectively; while the last term describes the added or removed heat to or from the adsorber by the heat transfer fluid (HTF).

The heat balance for the condenser could be written as:

$$\left(m_{ref}.C_{p_{ref}} + m_{Cu}.C_{p_{Cu}}\right)\frac{dT_{cond}}{dt} = -\delta m_{AC}\left[h_g\left(P_{cond}, T_{des}\right) - h_g\left(T_{cond}\right) + h_{fg}\right]\frac{dx_{des}}{dt} + \dot{m}_{w,cond}C_{p_w}\left(T_{w,in,cond} - T_{w,out,cond}\right) \quad (5)$$

The term on the left-hand side of Equation (5) describes the sensible heat rate of the refrigerant and metal within the condenser. The first term on the right hand-side simulates the heat that is generated by the condensation process. The last term represents the rate of the heat is absorbed by the HTF due to the condensation process. The outlet temperature of the heat transfer fluid from the condenser can be evaluated as shown in Equation (6):

$$T_{w,out,cond} = T_{cond} + \left(T_{w,in,cond} - T_{cond}\right)\exp\left(-\left(UA\right)_{cond}/\left(\dot{m}.C_p\right)_w\right) \quad (6)$$

The heat balance of the evaporator can be written as the following:

$$\left(m_{ref}.C_{p_{ref}} + m_{Cu}.C_{p_{Cu}}\right)\frac{dT_{evap}}{dt} = -\delta m_{AC}h_{fg}\frac{dx_{ads}}{dt} - \delta m_{AC}C_{p_{ref}}\left(T_{cond} - T_{evap}\right)\frac{dx_{des}}{dt} + \dot{m}_{Brine}C_{p_{Brine}}\left(T_{Brine,in} - T_{Brine,out}\right) \quad (7)$$

The term on the left-hand side of Equation (7) simulates the sensible heat rate of the refrigerant and metal within the evaporator. The first term on the right hand-side simulates the heat rate that is generated by the evaporation process; while the next term describes the heat quantity of vapour existing in the evaporator. The last term represents the rate heat is removed from the brine due to the evaporation process.

The outlet brine temperature was evaluated using Equation (8) as:

$$T_{Brine,cond} = T_{evap} + \left(T_{Brine,in} - T_{bed}\right)\exp\left(-\left(UA\right)_{evap}/\left(\dot{m}.C_p\right)_{brine}\right) \quad (8)$$

The heat balance of the integrated evaporator-condenser heat exchanger is given; as follows:

$$\left(m_{ref}.C_{p_{ref}} + m_{Cu}.C_{p_{Cu}}\right)\frac{dT_{cond/evap}^{bottom/upper}}{dt} = -\delta m_{AC}\left[h_g\left(P_{cond}, T_{des}\right) - h_g\left(T_{cond}\right) + h_{fg}\right]_{bottom} \frac{dx_{des}^{bottom}}{dt} - \delta m_{AC}\left[h_g\left(P_{evap}, T_{ads}\right) - h_g\left(T_{evap}\right) + h_{fg}\right]_{upper}\frac{dx_{ads}^{upper}}{dt} \quad (9)$$

The term on the left-hand side of Equation (9) determines the sensible heat rate of the refrigerants and metal of the IECHE. The first term on the right-hand side denotes heat rejected during the condensation process of the bottom cycle; while the last term simulates the latent heat required for the evaporation process of the upper cycle.

The cooling capacity of the system is evaluated only at the evaporator of the bottom (stage 2) cycle using the brine side during the whole cycle time, including the switching time.

$$Q_{evap}^{Bottom} = \left(1/t_{cycle}\right)\dot{m}_{Brine}C_{p\,Brine}\int_0^{tcycle}\left(T_{Brine,in} - T_{Brine,out}\right)dt\Big|_{Bottom,cycle} \qquad (10)$$

The rate of heat consumption during the preheating and desorption processes are evaluated for the upper and bottom cycles as the following:

$$Q_{heating}^{Upper\,/\,Bottom} = \left(1/t_{cycle}\right)\dot{m}_{w,hot}C_{p_{w,hot}}\int_0^{tcycle}\left(T_{hot,w,in} - T_{hot,w,out}\right)dt\Big|_{Upper\,/\,Bottom} \qquad (11)$$

The coefficient of the performance of the system:

$$COP = Q_{evap}^{Bottom}\,/\left(Q_{heating}^{Upper} + Q_{heating}^{Bottom}\right) \qquad (12)$$

Fig. 2 shows a flow chart of the Simulink/MATLAB model of the four bed cascaded adsorption system using the ICEHE. Simulink has been utilized to model the transient operation of the cascaded adsorption

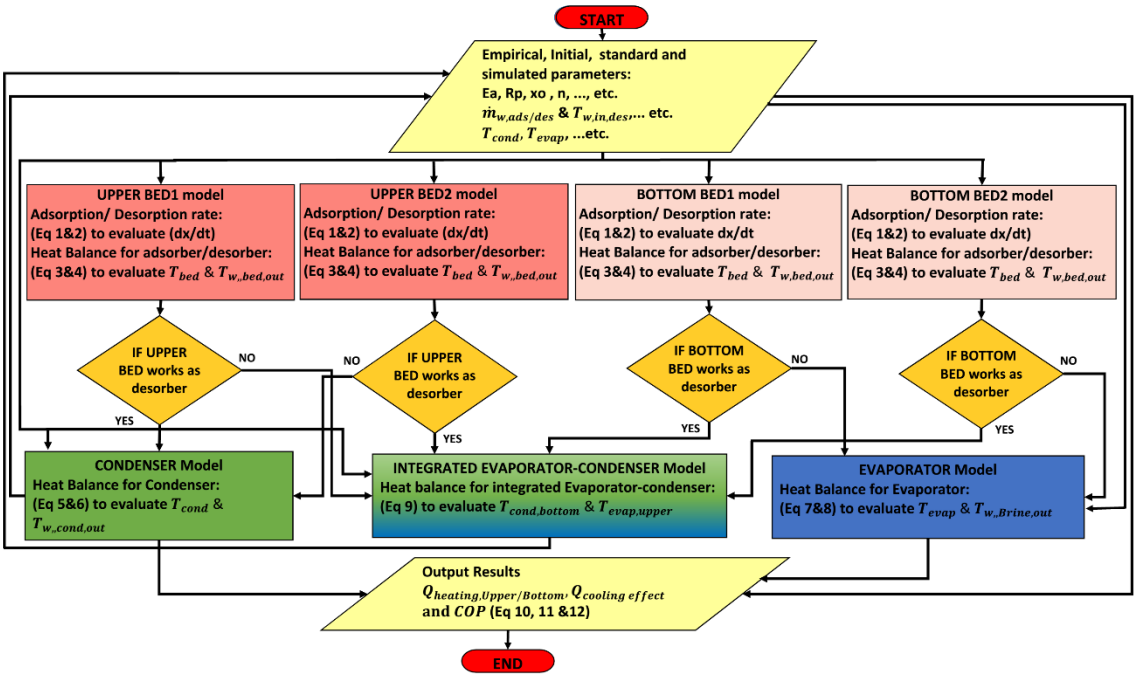

system. It is a dynamic solver which has many built-in commands and signal blocks that can be used directly and reduces the requirements for user coding, especially for complicated control systems [21].

Fig.2. Flow chart of cascading ice-making system model developed in Simulink

4. Validation of the Simulink Model and Results

The model has been validated using the results of Habib et al. [15] at the testing condition summarized in Table 1 using Maxsorb/R507A in the bottom cycle and Maxsorb/R134a in the upper cycle. The initial conditions for the different working pairs are determined using the pressure-temperature-uptake (PTX) diagram [15, 21-23]. Fig. 3 shows the good agreement of the predicted temperature profiles with ±6% deviation in the evaporator's temperature, ±2.7% in the condenser temperature, ±3.6% in the upper cycle beds' temperature and ±1.3% in the bottom cycle beds' temperature.

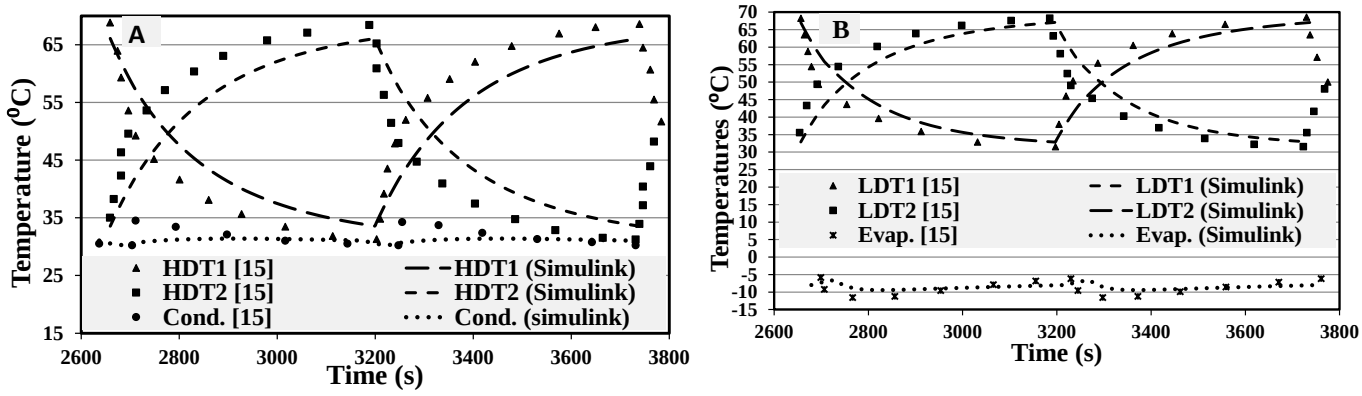

Fig.3. Validation of temperatures' trends with Habib's work: **(A)** of Maxsorb/R134a cycle **(B)** Maxsorb/R507A

Fig. 4A,B,C,D and E show the brine inlet and outlet temperatures and the cooling capacity variation with time for the different working pairs used in this work, with operating conditions shown in Table 2 and a half cycle time of 540 s. It can be seen that the drops in the outlet brine temperatures are 1.8, 0.7, 0.25, 3 and 1.7 K, respectively. Fig. 4D shows that the highest cooling capacity was achieved by

Maxsorb/R134a + Maxsorb/propane due to the latent heat of the evaporation of the propane being 2.28 times higher than that of R507A. Moreover, the operating pressure of R134a is higher than that of ethanol, which offers a good response in the adsorption process. The second highest cooling capacity was offered by ATO/ethanol + AC-35/methanol (Fig. 4E) followed by that of Maxsorb/134a +Maxsorb/507A (Fig. 4A), with an average cooling capacity of 1.1 kW and 0.8 kW being achieved, respectively. Although Maxsorb has an advantage in terms of higher adsorption capacity with refrigerants, compared to the ATO and AC-35, the higher cooling capacity of ATO/ethanol + AC-35/methanol is due to the higher latent heat of methanol and ethanol than that of R507A and R134a, by about 7.2 and 4.6 times, respectively at -8 ^{o}C.

The ATO/ethanol + Maxsorb/propane (Fig. 4B) and ATO/ethanol + Maxsorb/R507A (Fig. 4C) produce the lowest cooling capacity of 0.35 kW and 0.48 kW respectively. Therefore, the ATO/ethanol + AC-35/methanol system is selected to be described in detail. Fig. 4E presents the transient behaviour of the cooling capacity, inlet and outlet brine temperatures during the single cycle time in the evaporator. During the switching time, as there is no refrigerant circulating from the evaporator to the adsorber, the outlet brine temperature increases to reach a peak value at the end of this period. When the adsorber is linked with the evaporator, the adsorption process starts and the outlet brine temperature decreases gradually to reach steady state after 85 s and then rises slightly until the end of this process. The average difference

between the outlet and inlet brine temperature is about 1.2°C; the peak of the outlet brine temperature is synchronized with the drop in the cooling capacity as well. The difference in the cooling capacity is due to the variation of the adsorption properties. Based on the average brine outlet temperature in this research (-7 to -9.5°C), the current work could be used in cooling applications such as the medicine and food storage [20, 29], chemical engineering processes [20], thermal energy storage [30] and freeze desalination [31, 32].

Fig.4. (A),(B),(C),(D) & (E). Dynamic behaviour of cooling capacity, inlet and outlet brine temperature

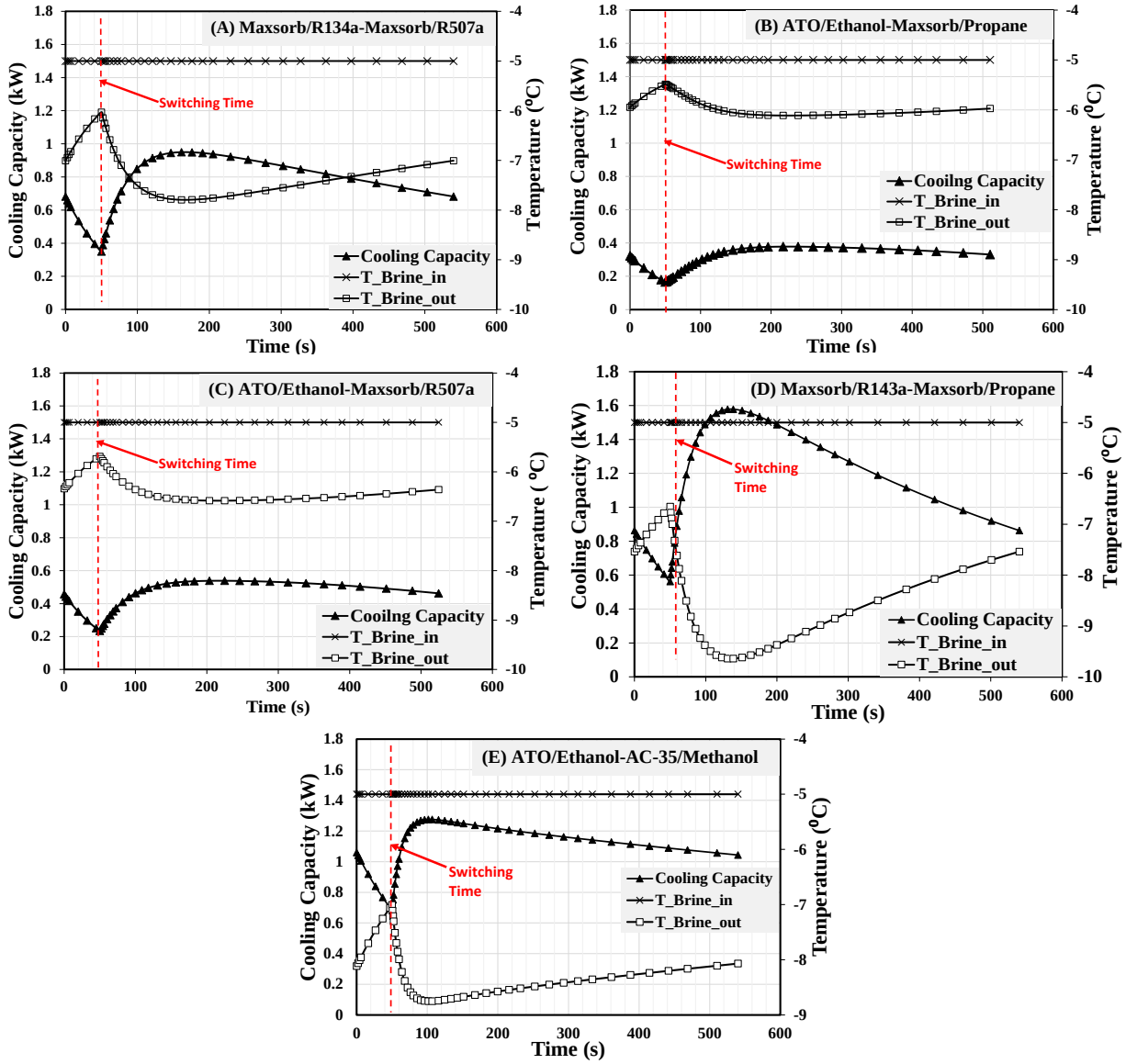

for five combinations of working pairs.

Fig. 5 shows the temperatures' variation with time for ten cycles of the ATO/ethanol-Maxsorb/propane working pairs' combination; where the temperatures' distribution of the HDT1, HDT2, condenser and the evaporator of the ICEHE are presented in Fig. 5A; and those of LDT1, LDT2, the condenser of the ICEHE and evaporator are indicated in Fig. 5B. The steady state condition for both cycles was reached after the third cycle at 3240 s at which the kinetic behavior of the adsorbent is changed from a dry condition to cyclic. Regarding the ICEHE, the average temperature of the evaporator and condenser is around 16 and 25^{o}C, respectively; which means that the integrated heat exchanger could be used simultaneously as a condenser for the bottom cycle and as an evaporator for the upper cycle.

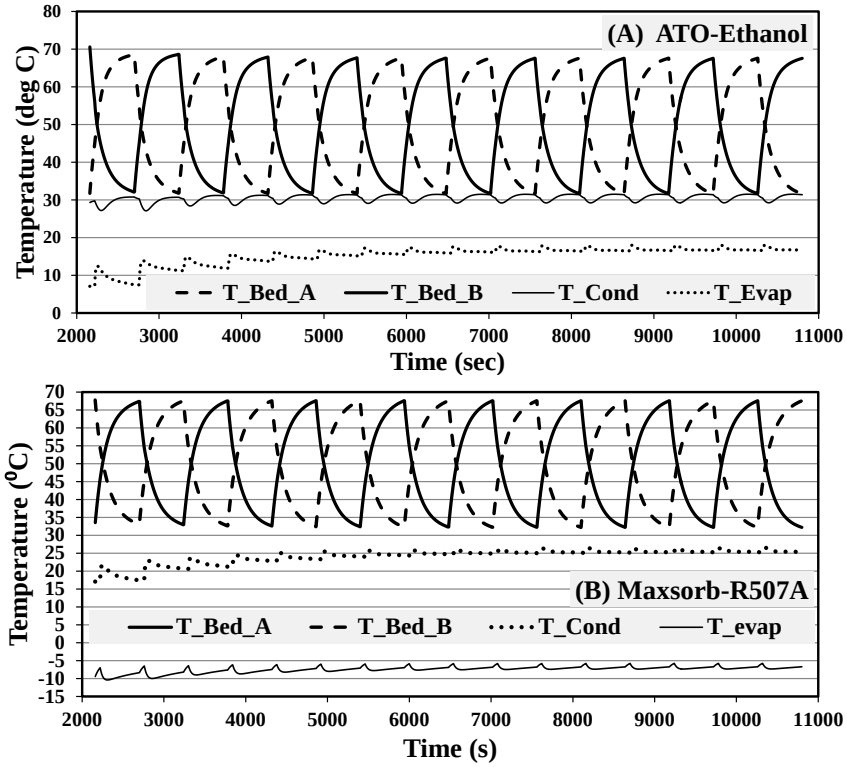

Fig. 5. Temperature distribution of the main parts of: (A) ATO/ethanol (B) Maxsorb/propane

Fig. 6 compares the cooling load of the five working pairs' combinations showing that the highest cooling capacity is produced by Maxsorb/R134 + Maxsorb/propane with up to 1.8 kW at a cycle time of 350

seconds. The ATO/ethanol + Maxsorb/propane and ATO/ethanol + Maxsorb/R507A produced similar a cooling output at all cycle times except for the cycle time of 1800 seconds. Also Fig. 6 shows that as the cycle time increases, the cooling output decreases for all the working pairs. The Maxsorb/R134a + Maxsorb/propane system produced the lowest brine temperature of -11.7^{o}C with the highest cooling capacity of 1.8kW. This could be due to the high latent heat of evaporation of propane compared to R507A and high pressure of R134a compared to ethanol which enables it to penetrate into the adsorbent pores effectively. Fig. 7 compares the COP of the cascaded system with the five adsorption pair combinations showing that Maxsorb/R134 + Maxsorb-propane produces the highest COP values among all the combinations used. However, as the cycle time decreases, the COP decreases. The second highest COP was produced by ATO/ethanol + AC-35/methanol with the difference ranging from 30% at low

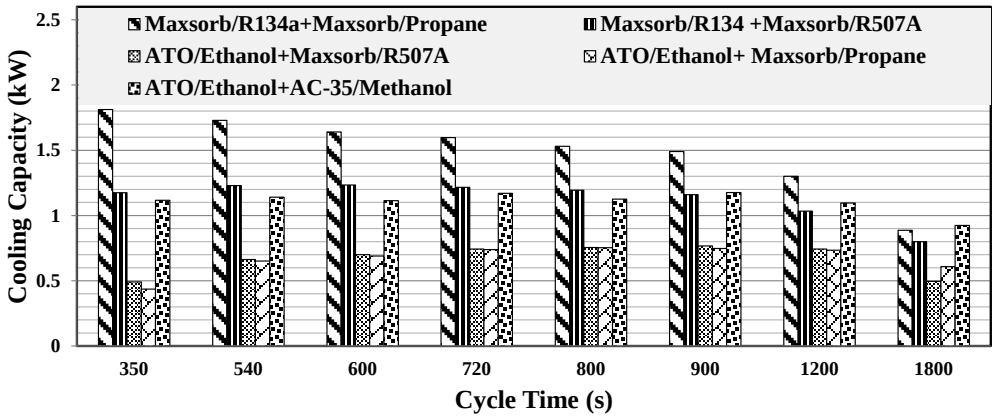

cycle time to 5% at the highest cycle time.

Fig.6. The effect of cycle time on the cooling capacity for different working pairs

Fig.7. The effect of cycle time on the COP for different working pairs

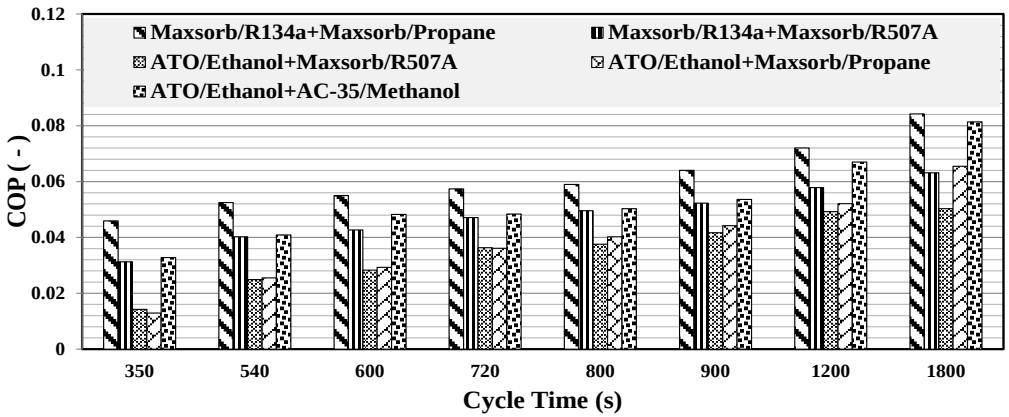

Parametric studies were investigated on ATO/ethanol + AC-35/methanol during the steady state condition for the second half of the cycle time after 13 cycles. The main purpose of these studies is to highlight the reasons for the low performance of the current system. as follows:

Fig. 8A shows the variation of the evaporator's temperature with time for different inlet brine temperatures. The figure shows that an evaporator temperature drop of 2, 1.7 and 1 K are produced at inlet brine temperatures of 0, -5 and -10 ^{0}C, respectively; resulting in lower cooling capacity and lower COP values as shown in Fig. 8B. This figure shows a fall in cooling capacity and COP by 52.5% and 46.3% as the inlet brine temperature decreased from 0 to -10^{0}C, respectively. The decreasing in the adsorption process of the refrigerant within the evaporator leads to this fall. In the current study, the selected brine temperature was -5 ^{0}C according to the required ice-making application and reasonable

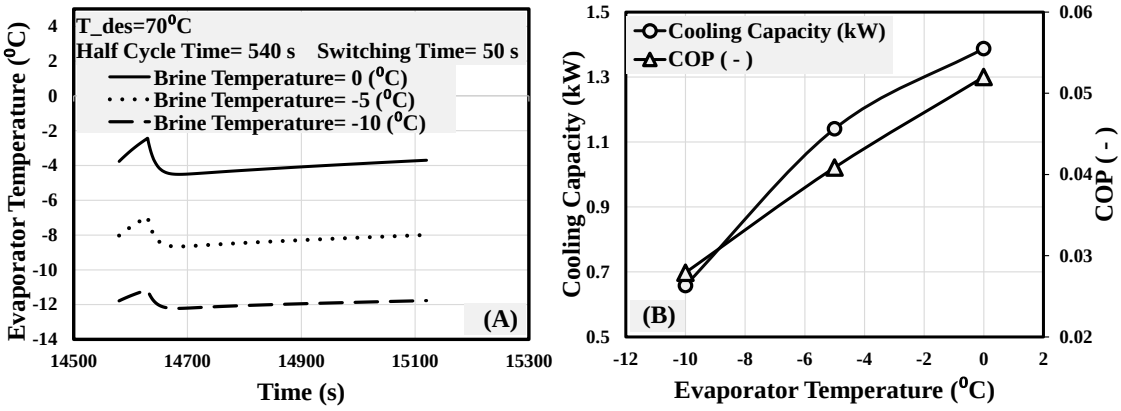

cooling capacity of 1.14 kW, compared to 0.65 at -10 ^{0}C.

Fig. 8. (A)&(B). Effect of inlet brine temperature on the evaporator's temperature, cooling capacity and COP

Fig. 9A shows the effect of the desorption temperature on the temperature histories of the evaporator. The figure shows that the drop in the evaporator's temperature increases from 1.7, 3.8 and 6.55 K as the desorption temperature increases from 70, 80 and 90 ^{0}C, respectively. The lower desorption temperature was simulated in the current work to exploited the low heat source as much as possible. The low

desorption temperature leads to a lower performance (see Fig. 9B), as a lower mass of refrigerant will be desorbed and condensed in the condenser resulting in lower refrigerant evaporation in the evaporator. Fig. 9B shows that there was a 73 and 56.2 % reduction in cooling capacity and COP when the desorption temperature decreased from 90 to 70^{0}C, respectively.

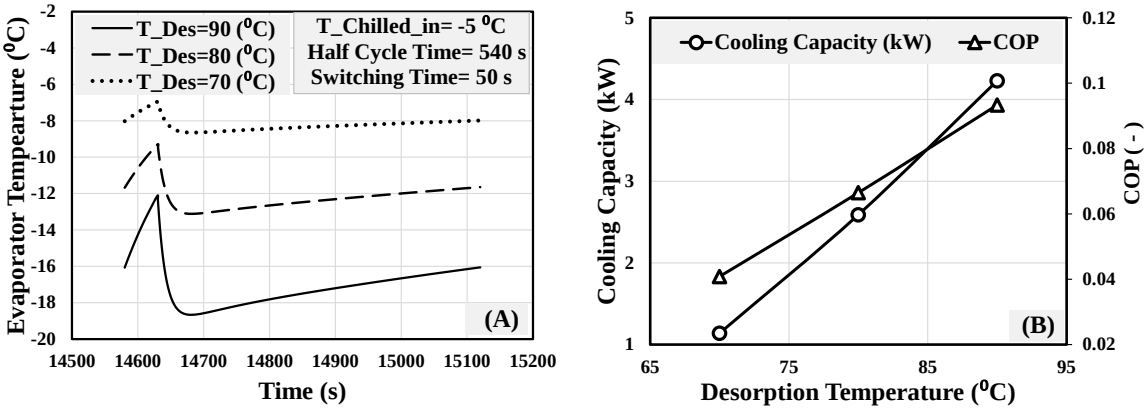

Fig. 9. (A)&(B). Effect of desorption temperature on the evaporator's temperature, cooling capacity and COP

Fig. 10A shows the evaporator's temperature histories simulated at three values of the condenser's temperatures. It is clear that as the condenser's temperature increases from 20, 25 and 30^{0}C, the drop in the evaporator's temperatures decreases from 3.13, 2.66 and 1.7 K, respectively. This can be explained by the reduced amount of refrigerant condensed at the higher condenser temperature, which leads to less refrigerant flowing to the evaporator. Fig. 10B shows the effect of increasing the condenser's temperature from 20^{0}C to 30^{0}C on cooling capacity and COP, where a decline in cooling capacity and COP up to 47.6% and 38.3%, respectively were found. Therefore increasing the condensation temperature, reducing the desorption temperature and reducing the evaporator's temperature result in reducing the system's performance.

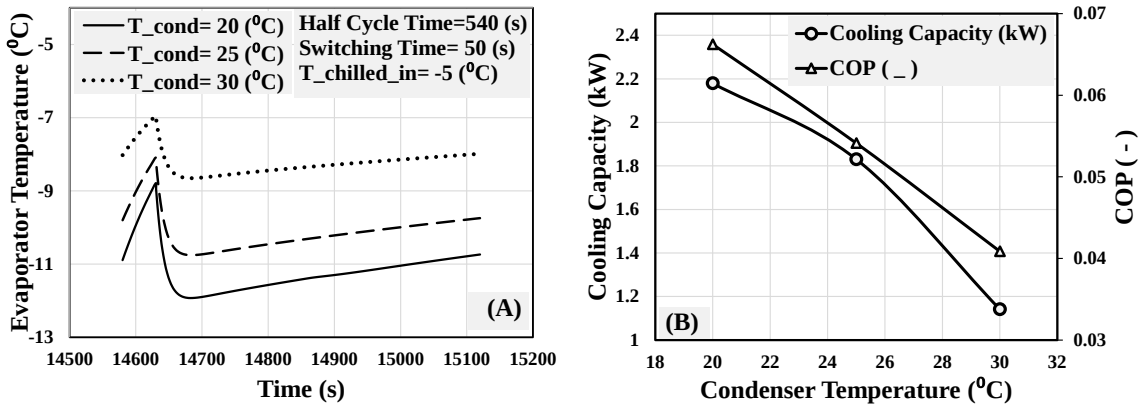

Fig. 10. (A) & (B). Effect of condenser's temperature on the evaporator's temperature, cooling capacity and COP

5. Conclusion

There is a significant amount of waste heat from power generation and industrial processes at temperatures below 100°C. The exploitation of such this waste heat can lead to a significant reduction of fossil fuel consumption and CO_2 emissions. Cascaded adsorption systems can exploit this waste heat to provide low temperature cooling for ice making. This work investigated different working pairs in an adsorption cascaded system consisting of four adsorbers, one condenser, an evaporator and an integrated evaporator-condenser heat exchanger for low temperature (-8°C) cooling. Five combinations of adsorbent-adsorbate have been investigated using Simulink/MATLAB, namely: ATO/ethanol + Maxsorb/R507A; Maxorb/R134a + Maxorb/propane; ATO/ethanol + Maxorb/propane; Maxorb/R134a + Maxsorb/R507A; and ATO/ethanol+AC-35/methanol. The results showed that Maxsorb/R134a+Maxsorb/propane has the best performance, in terms of COP (0.08) and cooling capacity (1.82 kW), compared to the other tested working pairs; this is due to the high latent heat of propane and high pressure of R134a and the Maxsorb's high adsorption characteristics. Also, the results showed that the ATO/ethanol+AC-35/methanol produced the second highest performance but with a significantly lower adsorbent material cost and with using environmentally friendly refrigerant. Based on the cost, the

combination of ATO/ethanol+AC-35/methanol offers a saving of up 13 times that of Maxorb/R134a + Maxsorb/R507A and Maxorb/R134a + Maxorb/propane. The only concern is safety; the methanol is a poisonous refrigerant so it is important to take in to account that an alarm sensor needs to be installed within the system. Although the results showed that this cascaded adsorption system with the proposed pairs can exploit waste heat sources with temperature as low as 70^{o}C, it has low COP (around 0.04) due to using a low heat source temperature, low evaporation and a high condensation temperature.

Acknowledgements

The authors would like to thank The Higher Committee for Education Development in Iraq (HCED) for sponsoring the project.

References

[1] Khan MZI, Alam KCA, Saha BB, Hamamoto Y, Akisawa A, Kashiwagi T. Parametric study of a two-stage adsorption chiller using re-heat—The effectof overall thermal conductance and adsorbent mass on system performance. International Journal of Thermal Sciences. 2006 Sep 19;45: 511–9.

[2] Oregon State University [Internet]. Oregon: Microwave ovens a key to energy production from wasted heat [updated 2011 Sep 20; cited 2015 August 10]. Available from: http://oregonstate.edu/ua/ncs/archives/2011/sep/microwave-ovens-key-energy-production-wasted-heat

[3] Hirota Y, Sugiyama Y, Kubota M, Watanabe F, Kobayashi N, Hasatani M, et al. Development of a suction-pump-assisted thermal and electrical hybrid adsorption heat pump. Applied Thermal Engineering. 2008 Sep;28(13):1687-93.

[4] Da Vinci Co., Ltd [Internet]. Japan: Rotary heat engine (RHE) [cited 2015 August 10] Available from: http://www.davinci-mode.co.jp/e/rhe.html

[5] Rezk A, AL-Dadah R, Mahmoud S, Elsayed A. Investigation of Ethanol/metal organic frameworks for low temperature adsorption cooling applications. Applied Energy. 2013 July 17; 112: 1025–31.

[6] Li, C., Wang, R.Z., Wang, L.W., Li, T.X. & Chen, Y. (2013). Experimental study on an adsorption icemaker driven by parabolic trough solar collector. Renewable Energy, 57, 223-33.

[7] Best R, Islas J, Martinez M. Exergy efficiency of an ammonia-water absorption system for ice production. Applied Energy. 1993;45:241-56.

[8] Garimella S, Brownb AM, Nagavarapua AK. Waste heat driven absorption/vapor-compression cascade refrigeration system for megawatt scale, high-flux,low-temperature cooling. International Journal of Refrigeration. 2011 June 2;34:1776-85.

[9] Wang D, Zhang J, Tian X, Liu D, Sumathy K. Progress in silica gel–water adsorption refrigeration technology. Renewable and Sustainable Energy Reviews. 2014 Feb;30:85–104.

[10] Khan MZI, Alam KCA, Saha BB, Akisawa A, Kashiwagi T. Study on a re-heat two-stage adsorption chiller – The influence of thermal capacitance ratio, overall thermal conductance ratio and adsorbent mass on system performance. Applied Thermal Engineering. 2007 Jul;27(10):1677–85.

[11] Wang R., Wang, L., Wu, J. Adsorption Refrigeration Technology: Theory and Application. 1st ed. China: John Wiley & Sons Singapore Pte. Ltd.; 2014.

[12] Meunier F. Second law analysis of a solid adsorption heat pump operating on reversible cascade cycles: application to the zeolite-water pair. Heat Recovery Systems. 1985;5(2):133-41.

[13] Akahira A, Alam KCA, Hamamoto Y, Akisawa A, Kashiwagi T. Mass recovery four-bed adsorption refrigeration cycle with energy cascading. Applied Thermal Engineering. 2005 Aug;25(11-12): 1764–78.

[14] Critopha RE. Adsorption refrigerators and heat pumps. In: Burchell TD, editor. Carbon materials for advanced technologies. 1st ed. USA: PERGAMON; 1999.p. 303-39.

[15] Habib K, Saha BB, Chakraborty, A, Koyama S, Srinivasan K. Performance evaluation of combined adsorption refrigeration cycles. International Journal of Refrigeration. 2011 Jan;34: 129-37.

[16] Meunier F. Theoretical performances of solid adsorbent cascading cycles using the zeolite-water and active carbon-methanol pairs: four case studies. Heat Recovery Systems. 1986;6(6): 491-98.

[17] Dawoud B. A hybrid solar-assisted adsorption cooling unit for vaccine storage. Renewable Energy 2007 May;32(6): 947–64.

[18] Oliveira RG, Silveira Jr V, Wang RZ. Experimental study of mass recovery adsorption cycles for ice making at low generation temperature. Applied Thermal Engineering. 2006 Feb; 26(2-3):303-11.

[19] Wang J, Wang LW, Luo WL, Wang RZ. Experimental study of a two-stage adsorption freezing machine driven by low temperature heat source. International Journal of Refrigeration. 2013;36: 1029-36.

[20] Jiang L, Wang LW, Wang RZ, Gao P, Song FP. Investigation on cascading cogeneration system of ORC (Organic Rankine Cycle) and CaCl2/BaCl2two-stage adsorption freezer. Energy. 2014;71: 377-87.

[21] Elsayed A, Al-Dadah R, Mahmoud S, Elshaer A, Bowen J. Investigation of Efficient Adsorbents Using Transient Analysis of Adsorption Chillers with Simulink. Proceedings of the International Conference on Heat Transfer and Fluid Flow; 2014 Aug 11-12. Prague, Czech Republic: International ASET Inc. 2014. P. 1-8.

[22] Ismail AB, Experimental and theoretical studies on adsorption chillers driven by waste heat and propane. [dissertation]. Singapore: National University of Singapore; 2013.

[23] Soong LW. [dissertation]. Experimental and theoretical studies of waste heat driven pressurized adsorption chillers. Singapore: National University of Singapore; 2010.

[24] El-Sharkawy, II, Kuwahara, K, Saha BB, Koyama S, Ng KC, Experimental investigation of activated carbon fibers/ethanol pairs for adsorption cooling system application. Applied Thermal Engineering. 2006;26(8-9):859–65.

[25] A&J Vacuum Services, Inc [Internet]. United State: Edwards Vacuum [cited 2016 January 1] Available from: http://www.ajvs.com/charcoal-ac35-steam-activated-carbon-pack-3-kg-for-edwards-vacuum-itc20k-itc-20k-vacuum-pump-inlet-chemical-trap-h12205002-7517.

[26] Himeno S, Komatsu T, Fujita S, High-Pressure Adsorption Equilibria of Methane and Carbon Dioxide on Several Activated Carbons. J. Chem. Eng. Data 2005; 50:369-376.

[27] Zhao Y, Hu E, Blazewicz A. Dynamic modelling of an activated carbon–methanol adsorption refrigeration tube with considerations of interfacial convection and transient pressure process. Applied Energy. 2012; 95:276-84.

[28] Gordeeva L, Aristov Y. Dynamic study of methanol adsorption on activated carbon ACM-35.4 for enhancing the specific cooling power of adsorptive chillers. Applied Energy. 2014;117:127-33.

[29] Song FP, Gong LX, Wang LW, Wang RZ. Study on gradient thermal driven adsorption cycle with freezing and cooling output for food storage. Applied Thermal Engineering. 2014;70:231-9.

[30] HanY, Shen B, Hu H, Fan F. Optimizing the performance of ice-storage systems in electricityload management through a credit mechanism: An analytical work for Jiangsu, China. The 6th International Conference on Applied Energy, Energy Procedia. 2014;61:2876-79.

[31] Lu Z, Xu L. Freezing desalination process. In: Thermal desalination processes – Vol. II - Encyclopedia of Desalination and Water Resources (DESWARE).

[32] Youssef PG, AL-Dadah RK, Mahmoud SM. Comparative Analysis of Desalination Technologies. The 6th International Conference on Applied Energy, Energy Procedia. 2014;61:2604-07.

Highlights

- Five combinations of working pairs with cascading adsorption system are simulated.
- Integrated evaporator- condenser heat exchanger is simulated with the stated system.
- The low-temperature heat source is applied to drive the adsorption refrigeration system.
- Natural refrigerants are investigated as one of the requirements of this work.
- ATO/Ethanol + AC-35/Methanol showed a good performance with the lowest cost.